

Vector Spatiotemporal Solitons and Their Memory Features in Cold Rydberg Gases

Yuan Zhao(赵元)^{1†}, Yun-Bin Lei(雷允彬)^{1†}, Yu-Xi Xu(徐羽茜)², Si-Liu Xu(徐四六)^{1*},
Houria Triki³, Anjan Biswas^{4,5}, and Qin Zhou(周勤)^{6*}

¹*School of Electronic and Information Engineering, Hubei University of Science and Technology, Xianning 437100, China*

²*School of International Education, Wuhan University of Technology, Wuhan 430071, China*

³*Radiation Physics Laboratory, Department of Physics, Faculty of Sciences, Badji Mokhtar University, P. O. Box 12, 23000 Annaba, Algeria*

⁴*Department of Physics, Chemistry and Mathematics, Alabama A&M University, Normal, AL 35762-4900, USA*

⁵*Mathematical Modeling and Applied Computation (MMAC) Research Group, Department of Mathematics, King Abdulaziz University, Jeddah 21589, Saudi Arabia*

⁶*School of Mathematical and Physical Sciences, Wuhan Textile University, Wuhan 430200, China*

(Received 27 December 2021; accepted 26 January 2022; published online 1 March 2022)

We propose a scheme to generate stable vector spatiotemporal solitons through a Rydberg electromagnetically induced transparency (Rydberg-EIT) system. Three-dimensional vector monopole and vortex solitons have been found under three nonlocal degrees. The numerical calculation and analytical solutions indicate that these solitons are generated with low energy and can stably propagate along the axes. The behavior of vector spatiotemporal solitons can be manipulated by the local and nonlocal nonlinearities. The results show a memory feature as these solitons can be stored and retrieved effectively by tuning the control field.

DOI: 10.1088/0256-307X/39/3/034202

Higher-dimensional spatiotemporal solitons (STSs) have attracted a lot of interest in many fields.^[1–8] In nonlinear optics, spatiotemporal solitons are unstable in Kerr media due to the Kerr nonlinearity.^[9,10] To reduce this rapid distortion, short pulses with high powered lasers were commonly applied in experiments to generate solitons.^[11,12] As these high energy solitons are hard to manipulate in optical information processes, there is another way to generate solitons with low energies. Moreover, the solitons with low energy are found to have memory features, and the storage and retrieval of these solitons are possible.^[13]

A number of optical systems have been proposed to satisfy these demands in theoretical and experimental studies.^[14–19] For example, Edmundson and Skryabin demonstrated a robust bistable STS with quadratic nonlinearities.^[14,15] Desyatnikov *et al.* and Ge found STSs in an optical media with higher order nonlinearities.^[16,17] Mihalache *et al.* obtained stable spinning STSs by tuning the focusing and defocusing nonlinearities.^[18] Zhang *et al.* revealed that 3D solitons can stably exist in atomic systems with spin-orbit coupling interactions.^[19] Systems with Rydberg atoms are proven to be an effective media to generate

stable solitons with low energies for the strong and long-range optical nonlinearities between the Rydberg atoms.^[20–25] Ultra-cold Rydberg atoms in a Bose-Einstein condensate is the latest hot topic of research for finding stable solitons with novel characters.^[26–29]

Despite the above progress, realizing single 3D vector STSs in Rydberg atomic systems is an open question. We focus on this question and present a systematic method to generate low power, stable spatiotemporal solitons with local Kerr nonlinearity and nonlocal nonlinearity.

Model. A 5-level Rydberg atomic system is constructed in Fig. 1(a). Four laser fields are coupled to this 5-level atomic system. A double Λ -type EIT configuration is constructed by states $|1\rangle$, $|2\rangle$, $|3\rangle$, $|4\rangle$, the probe (Ω_p), signal (Ω_s) and control (Ω_c) fields; $|5\rangle$ is coupled to $|4\rangle$ through auxiliary laser field Ω_a . In our work, the strontium (⁸⁸Sr) atomic gas is chosen as a potential atom to realize the system.^[30–32] The states above are $|1\rangle = |5S_{1/2}, F = 1, m_F = -1\rangle$, $|2\rangle = |5S_{1/2}, F = 2, m_F = 1\rangle$, $|3\rangle = |5S_{1/2}, F = 2, m_F = -1\rangle$, $|4\rangle = |5S_{1/2}, F = 2P_{3/2}, m_F = -1\rangle$, and $|5\rangle = |nS_{1/2}\rangle$. The main quantum number is $n = 60$.

The Hamiltonian of this 5-level Rydberg atomic system is $\hat{H}_H(t) = N_a \int_{-\infty}^{+\infty} d^3\mathbf{r} \hat{H}_H(\mathbf{r}, t)$, where N_a is

[†]These authors contributed equally to this work.

*Corresponding authors: xusiliu1968@163.com; qinzhou@whu.edu.cn

© 2022 Chinese Physical Society and IOP Publishing Ltd

atomic density. In the interaction picture, the Hamiltonian density is written as

$$\begin{aligned} \hat{H}_H(\mathbf{r}, t) = & \sum_{j=1}^4 \hbar \Delta_j \hat{S}_{jj}(\mathbf{r}, t) - \hbar \left[\Omega_p \hat{S}_{14}(\mathbf{r}, t) \right. \\ & \left. + \Omega_a \hat{S}_{45}(\mathbf{r}, t) + \Omega_s \hat{S}_{24}(\mathbf{r}, t) + \Omega_c \hat{S}_{34}(\mathbf{r}, t) + \text{H.c.} \right] \\ & + N_a \int_{\mathbf{r}' \neq \mathbf{r}} d^3 \mathbf{r}' \hat{S}_{55}(\mathbf{r}', t) \hbar V(\mathbf{r}' - \mathbf{r}) \hat{S}_{55}(\mathbf{r}, t), \end{aligned} \quad (1)$$

where $\hat{S}_{jl} = |l\rangle\langle j| \exp i[(\mathbf{k}_l - \mathbf{k}_j) \cdot \mathbf{r} - (\omega_l - \omega_j + \Delta_l - \Delta_j)t]$, $\Delta_2 = \omega_p - \omega_s - (\omega_2 - \omega_1)$, $\Delta_3 = \omega_p + \omega_c - (\omega_3 - \omega_1)$ and $\Delta_5 = \omega_p + \omega_a - (\omega_5 - \omega_1)$ are the two-photon detunings, $\Delta_4 = \omega_p - (\omega_4 - \omega_1)$. $\Omega_p = (\mathbf{e}_p \cdot \mathbf{p}_{41})\varepsilon_p/\hbar$, $\Omega_c = (\mathbf{e}_c \cdot \mathbf{p}_{43})\varepsilon_c/\hbar$, $\Omega_s = (\mathbf{e}_s \cdot \mathbf{p}_{42})\varepsilon_s/\hbar$ and $\Omega_a = (\mathbf{e}_a \cdot \mathbf{p}_{54})\varepsilon_a/\hbar$ are the half Rabi frequencies. Substituting the Hamiltonian to the optical Bloch equation $\partial\rho/\partial t = -i[\hat{H}, \rho]/\hbar - \Gamma[\rho]$, we can get the density equations of the system [see the Supplementary Material].

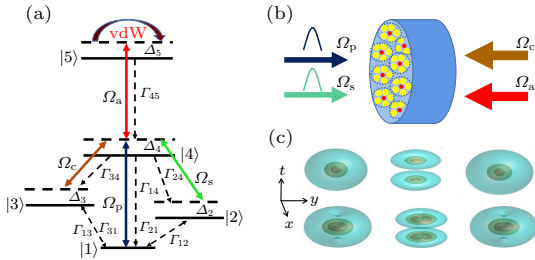


Fig. 1. (a) The 5-level Rydberg atomic system with double EIT configuration. States $|1\rangle$, $|2\rangle$, $|3\rangle$ and $|4\rangle$ constitute the double standard Λ -type EIT configurations. The probe/signal/control/auxiliary field ($\Omega_p/\Omega_s/\Omega_c/\Omega_a$) couple the transitions $|1\rangle \rightarrow |4\rangle$, $|2\rangle \rightarrow |4\rangle$, $|3\rangle \rightarrow |4\rangle$ and $|4\rangle \rightarrow |5\rangle$. Γ_{jl} is the spontaneous emission decay rates, Δ_j is the detuning. (b) Illustration of the system. (c) Storage and retrieval of monopole STSs (upper) and vortex STSs (lower) in the general nonlocal response, illustrated by isosurface plots of the intensity of vector STSs at $z = 0, 2L_{\text{diff}}, 4L_{\text{diff}}$, where L_{diff} is the diffraction distance.

The equation of motions for the Ω_p and Ω_s is governed by the Maxwell equation $\nabla^2 \mathbf{E} - (1/c^2)\partial^2 \mathbf{E}/\partial t^2 = [1/(\varepsilon_0 c^2)]\partial^2 \mathbf{P}/\partial t^2$, where $\mathbf{P} = N_a \text{Tr}(\rho \mathbf{p})$. Under slowly varying envelope approximation, the probe field Ω_p and signal field Ω_s satisfy

$$\begin{aligned} i \left(\frac{\partial}{\partial z} + \frac{1}{c} \frac{\partial}{\partial t} \right) \Omega_{p(s)} + \frac{1}{2k_{p(s)}} \left(\frac{\partial^2}{\partial x^2} + \frac{\partial^2}{\partial y^2} \right) \Omega_{p(s)} \\ + \kappa_{14(24)} \rho_{41(42)} = 0, \end{aligned} \quad (2)$$

where $k_{p(s)} = \omega_{p(s)}/c$, $\kappa_{14} = N_a k_p |\mathbf{p}_{14} \cdot \mathbf{e}_p|^2 / 2\varepsilon_0 \hbar$ and $\kappa_{24} = N_a k_s |\mathbf{p}_{24} \cdot \mathbf{e}_s|^2 / 2\varepsilon_0 \hbar$.

To obtain divergence-free solutions for the one- and two-body correlators of the order of magnitude in the density equations, we assume $\rho_{jl} \equiv \langle \hat{S}_{jl} \rangle$ and $\rho_{jl, \mu\nu} \equiv$

$\langle \hat{S}_{jl} \hat{S}_{\mu\nu} \rangle$. In order to solve these equations, the physical quantities are expanded as $\Omega_p = \sum_{m=1} \varepsilon^m \Omega_p^{(m)}$, $\Omega_s = \sum_{m=1} \varepsilon^m \Omega_s^{(m)}$, $\rho_{j1} = \sum_{m=0} \varepsilon^{2m+1} \rho_{j1}^{(2m+1)}$, $\rho_{jl} = \sum_{m=1} \varepsilon^{2m} \rho_{jl}^{(2m)}$, $\rho_{11} = 1 + \sum_{m=1} \varepsilon^{2m} \rho_{11}^{(2m)}$, $\rho_{j1, l1} = \sum_{m=1} \varepsilon^{2m} \rho_{j1, l1}^{(2m)}$, $\rho_{j1, 1l} = \sum_{m=1} \varepsilon^{2m} \rho_{j1, 1l}^{(2m)}$, $\rho_{jl, \mu 1} = \sum_{m=1} \varepsilon^{2m+1} \rho_{jl, \mu 1}^{(2m+1)}$, and $\rho_{jl, \mu\nu} = \sum_{m=2} \varepsilon^{2m} \rho_{jl, \mu\nu}^{(2m)}$ ($j, l, \mu, \nu = 2, 3, 4, 5$). The space and time scales are also expressed as $x_1 = \varepsilon x$, $y_1 = \varepsilon y$, $z_l = \varepsilon^l z$ ($l = 0, 1, 2$), and $t_l = \varepsilon^l t$ ($l = 0, 1$).^[13] Substituting these expansions into Maxwell's equation and Bloch's equation, we obtain the following solutions order by order.

At the zeroth and first order approximation, we get the Rabi frequencies $\Omega_p^{(1)} = F_1 e^{i\theta_p}$, $\Omega_s^{(1)} = F_2 e^{i\theta_s}$ with $\theta_p = K_p(\omega)z_0 - \omega t_0$, $\theta_s = K_s(\omega)z_0 - \omega t_0$. F_1 and F_2 are undetermined envelope functions, $K_p(\omega)$ and $K_s(\omega)$ are linear dispersion relations with

$$K_p(\omega) = \frac{\omega}{c} + \frac{\kappa_{14}}{D_1} [(\omega + d_{21})(\omega + d_{31})(\rho_{11}^{(0)} - \rho_{44}^{(0)}) + \Omega_c \rho_{43}^{*(0)}], \quad (3)$$

$$\begin{aligned} K_s(\omega) = \frac{\omega}{c} + \frac{\kappa_{24}}{D_2} [(\omega + d_{32})(\omega + d_{52})(\rho_{22}^{(0)} - \rho_{44}^{(0)}) \\ + (\omega + d_{52})\Omega_c \rho_{43}^{*(0)} + (\omega + d_{32})\Omega_a \rho_{54}^{*(0)}]. \end{aligned} \quad (4)$$

Here $D_{1(2)} = (\omega + d_{51(52)})|\Omega_c|^2 + (\omega + d_{31(32)})|\Omega_a|^2 - (\omega + d_{31(32)})(\omega + d_{41(42)})(\omega + d_{51(52)})$, $d_{jl} = \Delta_j - \Delta_l + i\gamma_{jl}$ ($i, j = 1, 2, 3, 4; i \neq j$), where $\gamma_{jl} = (\Gamma_j + \Gamma_l)/2 + \gamma_{ij}^{\text{dep}}$, $\Gamma_l = \sum_{j < l} \Gamma_{jl}$, γ_{ij}^{dep} is the dephasing rate; $\rho_{jl}^{(0)}$ and $\rho_{jl}^{(1)}$ ($j, l = 1, \dots, 5$), the density matrix elements in the zeroth and first order approximation are given detailedly in the Supplementary Material.

At the second order approximation, the envelope functions satisfy $i[\partial F_l / \partial z_1 + (1/V_{gl})\partial F_l / \partial t_1] = 0$ ($l = 1, 2$), where $V_{gl} = 1/K_l$ ($K_l = \partial K_j / \partial \omega$) ($j = p, s$) is group velocity. The laser field then has this expression $\psi_l = F_l \exp(-\mu_l z)$, where $\mu_l = \varepsilon^{-2} \text{Im}(K_l)$ is the absorption coefficient.

At the third and fourth orders, the probe and signal fields satisfy the dimensionless form

$$\begin{aligned} i \frac{\partial \psi_{1(2)}}{\partial s} + \left(\frac{\partial^2 \psi_{1(2)}}{\partial \xi^2} + \frac{\partial^2 \psi_{1(2)}}{\partial \eta^2} + \frac{\partial^2 \psi_{1(2)}}{\partial \tau^2} \right) \\ + (g_{11(22)} |\psi_{1(2)}|^2 + g_{12(21)} |\psi_{2(1)}|^2) \psi_{1(2)} \\ + \alpha \int d^3 r'_\perp G_2(r'_\perp - r_\perp) |\psi_{1(2)}|^2 \psi_{1(2)} = 0, \end{aligned} \quad (5)$$

where the units of the physical quantities are set to be 1. Here $\psi_{1(2)} = \Omega_{p(s)}/\Omega_{p(s)0}$ are dimensionless quantities, $\Omega_{p(s)0}$ is the initial frequency of the probe/signal pulse; $s = z/(2L_{\text{diff}})$, $(\xi, \eta) = (x, y)/R_0$, $\tau = t - z/V_g$, with $L_{\text{diff}} = 2\omega_p R_0^2/c$ and $R_{p0} = R_{s0} = R_0$ being the typical radius of the probe and signal pulses;

$\alpha = 2N_a R_0^2 |\psi_0|^2 L_{\text{diff}} / D(\omega)$ is the degree of nonlocality; $g_{jl} = -2W_{jl} |\Omega_0|^2 L_{\text{diff}}$ are the interaction coefficients, where W_{11} and W_{22} are the nonlinear self-focusing coefficients, W_{12} and W_{21} are the nonlinear cross-phase coefficients. The detail expressions of W_{jl} ($j, l = 1, 2$) are given in the Supplementary Material.

Three-Dimensional Vector Spatiotemporal Solitons and Their Memory Feature. In this study, we assume $\psi_{1(2)} = \psi_{1(2)} e^{i b s}$, where b is the propagation coefficient. Then the energies of solitary wave are $U_{1(2)} = \iint |\psi_{1(2)}|^2 d\xi d\eta$, and total energy is $U = U_1 + U_2$.

The eigenvalue of Eq. (5) can be obtained by using the numerical and analytical methods.^[33,34] With perturbation, we have $\psi_{1(2)} = [\psi_{01(2)} + (u_{1(2)} + v_{1(2)})e^{\lambda s} +$

$(u_{1(2)}^* - v_{1(2)}^*)e^{\lambda^* s}]e^{i b s}$, where $\psi_{0(1,2)}$ is the stationary solution of Eq. (5), $u_{1(2)}, v_{1(2)} \ll \psi_{01(2)}$ are the perturbation terms, and λ is a complex parameter indicating the perturbation growth rate. According to the criteria, the soliton solutions can be stable if $\text{Re}(\lambda) = 0$.^[35] The parameters we choose in this system are $R_{\perp} = 12 \mu\text{m}$, $\tau_0 = 1.1 \times 10^{-6} \text{s}$, $\Gamma_{21} = 0.21\pi \text{MHz}$, $\Gamma_4 = 2.2\pi \times 10^6 \text{MHz}$, $\Gamma_5 = \Gamma_{45} = 2\pi \times 16.9 \text{kHz}$, $\Delta_2 = 0.27 \times 10^6 \text{s}^{-1}$, $\Delta_3 = 1.68 \times 10^6 \text{s}^{-1}$, $\Delta_4 = 1.1 \times 10^8 \text{s}^{-1}$, $\Delta_5 = 2.37 \times 10^7 \text{s}^{-1}$, $N_a = 1.0 \times 10^{12} \text{cm}^{-3}$, $\Omega_c = \Omega_{c0} = 1.2 \times 10^7 \text{s}^{-1}$, $\Omega_a = \Omega_{a0} = 5 \times 10^6 \text{s}^{-1}$. In this case, the solitary wave is generated with small power $P_{1(2)} = 1.7 \text{nW}$, and propagates with very slow speed $V_{g_{1(2)}} \approx 2.47 \times 10^{-6} c$ (point B in Fig. 2).^[10]

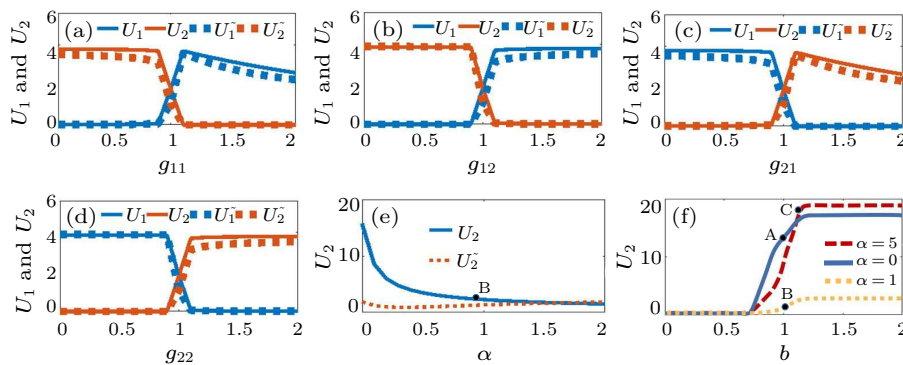


Fig. 2. (a)–(e) Energy flow of probe and signal pulses versus the relative local parameters g_{jl} ($j, l = 1, 2$) and nonlocal nonlinearity strength α . (f) U_2 – b relation with different α . The solid lines represent the numerical solutions, and the dotted lines are the analysis results. The other parameters are set to be 1, i.e., $g_{jl} = \alpha = 1$. Point A: $U_2 = 15$, $\alpha = 0$, $b = 1$. Point B: $U_2 = 1.4$, $\alpha = b = 1$. Point C: $U_2 = 18$, $\alpha = 5$, $b = 1.1$.

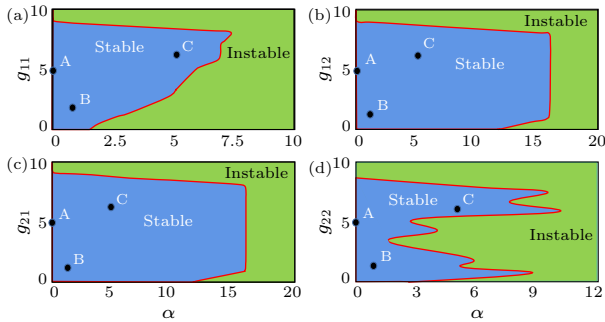


Fig. 3. (a)–(d) Stability areas for 3D vector STSs in the (g_{jl}, α) plane. The stable shaded regions appear in blue and unstable regions appear in green. Point A (local): $g_{jl} = 5$, $\alpha = 0$. Point B (general nonlocal): $g_{jl} = 1$, $\alpha = 1$. Point C (strongly nonlocal): $g_{jl} = 6$, $\alpha = 5$.

Figure 2 shows the energy of probe (U_1) or signal (U_2) pulses. In Figs. 2(a) and 2(b), one can see that U_2 initially decreases slowly with $g_{11(12)}$. When $g_{11(12)} > 0.92$, U_2 starts to drop rapidly, until nearly zero, and it remains constant. Nevertheless, U_1 increases rapidly to maximum, then it decreases slowly with $g_{11(12)}$. On the contrary, $U_{1(2)}$ – $g_{21(22)}$ relations in Figs. 2(c) and 2(d) show the opposite trends. Further, the total energies of two pulses stay almost the same,

as long as parameters α and b are not changed. The numerical solutions (solid lines) agree well with the analytical solutions (dotted line). Figure 2(e) shows the $U_{1(2)}$ – α relation, where only U_2 is plotted because U_1 overlaps with U_2 in the simulation. One can see that $U_{1(2)}$ decreases monotonously with α , so the total energy decreases when tuning α . Further, when $\alpha < 1.47$, there is a great difference between the analytical solution and the numerical simulation; however, they agree very well when $\alpha \geq 1.47$. In Fig. 2(f), U monotonically increases with b . According to the VK stability criterion, these vector STSs found here are stable when $dU/db > 0$.^[36] Further, we find that the larger the α , the larger the stability ranges vector STSs have.

Figure 3 shows the stability areas for 3D vector STSs in the (g_{jl}, α) plane with $j, l = 1, 2$. Numerical results display that vector STSs exist and are stable in the blue area. Simulation results show that five parameters (i.e., g_{11} , g_{12} , g_{21} , g_{22} , and α) profoundly affect the stability range of solitons. Comparing Figs. 3(a) and 3(d) with Figs. 3(b) and 3(c), we can find that the cross-phase modulation parameters (i.e., g_{12} and g_{21}) are more robust than the self-phase

modulation parameters (i.e., g_{11} and g_{22}).

Vector soliton solutions to Eq. (5) are given in three nonlocality degrees: (i) $R_b \ll R_0$ (local response region), (ii) $R_b \approx R_0$ (general nonlocal response region), and (iii) $R_b \gg R_0$ (strongly nonlocal response region), where R_b is the Rydberg blockade radius.^[37] The dynamical properties of 3D vector STSs in local (dot A), general nonlocal (dot B) and strongly nonlocal (dot C) response regions are plotted in Fig. 4. Three-dimensional monopole solitons (soliton energy distributes in the center with only one

peak) and vortex solitons (soliton energy distributes as a vortex profile with the smallest energy in the center) are both shown under a random perturbation. Note that monopole solitons are more stable than vortex solitons in our system in all three nonlocality degrees, which is similar to the existing reports.^[18,38,39] Comparing the stabilities of solitons in three nonlocality degrees, we find that 3D vector STSs in strongly nonlocal response region are the most stable ones. On the contrary, solitons in local response region are the most unstable ones.

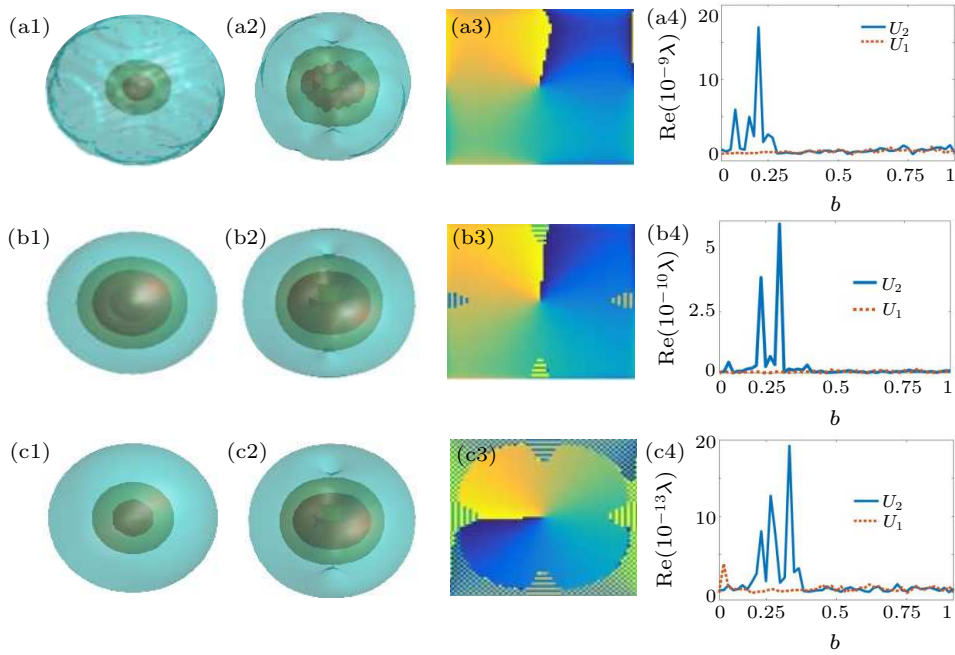


Fig. 4. Dynamical properties of 3D vector STSs in local (a1)–(a4), general nonlocal (b1)–(b4) and strongly nonlocal (c1)–(c4) response regions, corresponding to dots A, B and C in Figs. 2 and 3, respectively. Isosurfaces of 3D monopole STSs [(a1), (b1), (c1)] and vortex STSs [(a2), (b2), (c2)]. Phases of 3D vortex STSs [(a3), (b3), (c3)]. The first three columns are plotted under a random perturbation at $s = 27$. [(a4), (b4), (c4)] Linear-stability spectra of monopole and vortex STSs. Other parameters are the same as Fig. 3.

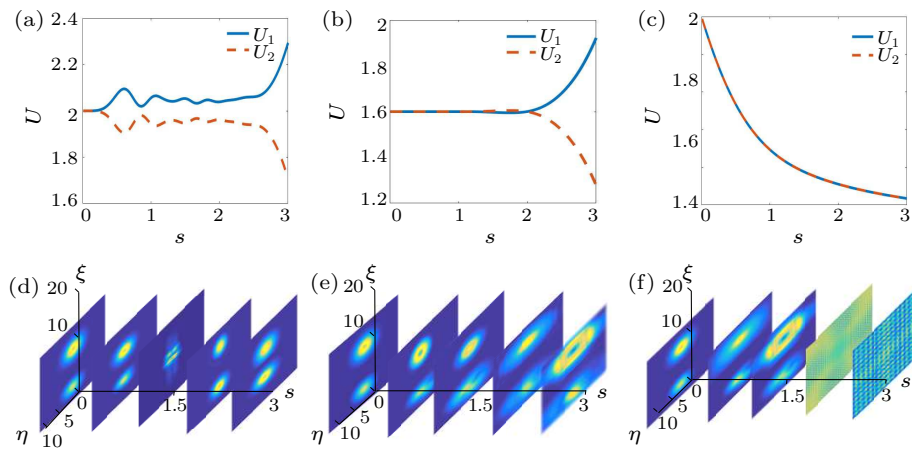


Fig. 5. (a)–(c) Energy flow of $|U_1|$ (i.e. monopole STSs, solid blue), and $|U_2|$ (i.e. vortex STSs, dashed red) at $s = 0, 3/4, 3/2, 9/4, 3$ with three nonlocal response regions. (d)–(f) Evolution of monopole STSs and the vortex STSs. [(a), (d)] Strongly nonlocal response. [(b), (e)] General nonlocal response, [(c), (f)] Local response. Other parameters are the same as Fig. 3.

The dynamics of vector STSs in this system may be tested by numerically solving Eq. (5) with the fast fractional Fourier algorithm.^[35] Figure 5 displays the evolution of vector STSs in strongly nonlocal [(a), (d)], general nonlocal [(b), (e)], and local [(c), (f)] response regions. Figures 5(a)–5(c) show the energy flows $|U_1|$ (monopole solitons) and $|U_2|$ (vortex solitons). One can see that the total energy of monopole and vortex solitons almost remains the same in both strongly nonlocal and general nonlocal response regions, although $|U_1|$ and $|U_2|$ show some oscillations with the propagation distance s in strongly nonlocal response region. When $s > 2.1$, $|U_1|$ suddenly increases and $|U_2|$ decreases. However, $|U_{1(2)}|$ and the total energy decrease with s in the local response region [see Fig. 5(c)].

Further, in strongly nonlocal response region, one can find a quasi-elastic collision phenomenon between monopole and vortex solitons in the propagation [see Fig. 5(d)]. The distribution of the vector STSs is basically unchanged, and the solitons remain stable after

the collision. This collision phenomenon is absent in the general nonlocal and local response region. The distribution of the vector STSs changes significantly in general nonlocal response region [Fig. 5(e)] and produces collapse in local response region [Fig. 5(f)].

Next, we investigate the memory feature of the solitons by modulating the control field. The control field has two states, switch-on and switch-off.^[40] The input probe and signal pulses are taken as a fundamental Gaussian mode and re^{-r^2} , respectively. The memory feature can be described by the efficiency η and fidelity ηJ^2 .

The storage and retrieval of the 3D vector STSs are shown in Figs. 1(c) and 6. Figure 1(c) display the numerical results of the intensity of the probe and signal pulse $U_{1(2)}/U_0$ during propagation. It is shown that 3D vector STSs can be stored and retrieved effectively by the switch-on and switch-off of the control field. There is still small deformation of the vector STSs, after storage, due to dissipation.

Table 1. The efficiency and fidelity of the memory effect.

Nonlocal degree	Monopole solitons		Vortex solitons	
	efficiency	fidelity	efficiency	fidelity
Local	0.80	0.70	0.75	0.71
General nonlocal	0.92	0.80	0.91	0.82
Strongly nonlocal	0.98	0.95	0.96	0.91

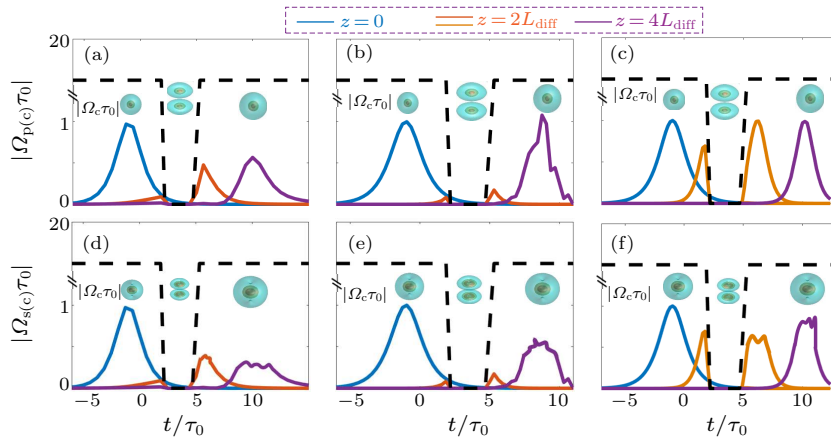


Fig. 6. Memory feature of 3D monopole STSs and vortex STSs in the local [(a), (d)], general nonlocal [(b), (e)] and strongly nonlocal [(c), (f)] response regions. The first row represents monopole STSs, and the second row represents vortex STSs. The black dashed line shows the switch-on, switch-off, and re-switch-on of the control field $|\Omega_c\tau_0|$. The blue, orange and purple lines are $|\Omega_{p(s)}\tau_0|$ at $z = 0$ (at the beginning), $z = 2L_{\text{diff}}$ (during the storage), and $z = 4L_{\text{diff}}$ (after the retrieval), with $L_{\text{diff}} = 1.37$ mm. Other parameters are the same as Fig. 2.

Figure 6 display the memory effects of monopole and vortex solitons in three nonlocal response regions. The efficiency and fidelity of the memory effect are given in Table 1. In the local response region [Figs. 6(a) and 6(d)], the vector STSs have a tremendous amount of deformation after storage due to the imbalance of diffraction, dispersion and nonlinearity. The efficiency and fidelity are relatively low for both monopole STSs and vortex STSs. In the general non-

local response region [Figs. 6(b) and 6(e)], one can see that after storage the vector STSs characterize a small amount of wave shape deformation. However, in the strongly nonlocal response region [Figs. 6(c) and 6(f)], the monopole STSs (vortex STSs) retain nearly the same wave shape after storage. Here, we obtain the highest efficiency and fidelity. One can see that the nonlocality is the critical factor in the storage and retrieval of the solitons.

In summary, we have proposed a 5-level Rydberg-EIT atomic system to generate stable vector spatiotemporal solitons. The formation, propagation, and stability analysis of 3D monopole and vortex solitons are studied. The vector STSs are proven to be stable and can be stored and retrieved effectively in nonlocal response region. Our study provides a new application of optical solitons in the optical information.

Acknowledgements. This work was supported by the Hubei Provincial Science and Technology Plan (Grant No. 2019BEC206), the Hubei Provincial Key Research and Development Plan (Grant No. 2020BGC028), the National Natural Science Foundation of China (Grant No. 11975172), Hubei University of Science and Technology (Grant No. 2020-22GP04).

References

- [1] Chen S L, Wang L X, Wen L, Dai C Q, Liu J K and Zhang X F 2021 *Optik* **247** 167932
- [2] Wang L L and Liu W J 2020 *Chin. Phys. B* **29** 070502
- [3] Yan Y Y and Liu W J 2021 *Chin. Phys. Lett.* **38** 094201
- [4] Zhou Q 2022 *Chin. Phys. Lett.* **39** 010501
- [5] Zhou Q, Wang T, Biswas A and Liu W J 2022 *Nonlinear Dyn.* **107** 1215
- [6] Cao Q and Dai C Q 2021 *Chin. Phys. Lett.* **38** 090501
- [7] Yin K, Cheng X P and Lin J 2021 *Chin. Phys. Lett.* **38** 080201
- [8] Zhao J, Luan Z, Zhang P, Dai C, Biswas A, Liu W and N A 2020 *Optik* **220** 165189
- [9] Silberberg Y 1990 *Opt. Lett.* **15** 1282
- [10] Bai Z Y, Li W and Huang G X 2019 *Optica* **6** 309
- [11] Minardi S, Eilenberger F, Kartashov Y V, Szameit A, Röpke U, Kobelke J, Schuster K, Bartelt H, Nolte S, Torner L, Lederer F, Tünnermann A and Pertsch T 2010 *Phys. Rev. Lett.* **105** 263901
- [12] Malomed B, Mihalache D, Wise F and Torner L 2005 *J. Opt. B* **7** R53-R72
- [13] Mcleod R, Wagner K and Blair S 1995 *Phys. Rev. A* **52** 3254
- [14] Edmundson D E and Enns R H 1992 *Opt. Lett.* **17** 586
- [15] Skryabin D V and Firth W J 1998 *Opt. Commun.* **148** 79
- [16] Desyatnikov A, Maimistov A I and Malomed B A 2000 *Phys. Rev. E* **61** 3107
- [17] Ge J J, Shen M, Ma C L, Zang T C and Dai L 2015 *Phys. Rev. E* **91** 023203
- [18] Mihalache D, Mazilu D, Crasovan L C, Towers I, Buryak A V, Malomed B A, Torner L, Torres J P and Lederer F 2002 *Phys. Rev. Lett.* **88** 073902
- [19] Zhang Y C, Zhou Z W, Malomed B A and Pu H 2015 *Phys. Rev. Lett.* **115** 253902
- [20] Hang C and Huang G X 2018 *Phys. Rev. A* **98** 043840
- [21] Friedler I, Petrosyan D, Fleischhauer M and Kurizki G 2005 *Phys. Rev. A* **72** 043803
- [22] Mohapatra A K, Jackson T R and Adams C S 2007 *Phys. Rev. Lett.* **98** 113003
- [23] Xu S L, Zhou Q, Zhao D, Belić M R and Zhao Y 2020 *Appl. Math. Lett.* **106** 106230
- [24] Gorshkov A V, Otterbach J, Fleischhauer M, Pohl T and Lukin M D 2011 *Phys. Rev. Lett.* **107** 133602
- [25] He B, Sharypov A V, Sheng J, Simon C and Xiao M 2014 *Phys. Rev. Lett.* **112** 133606
- [26] Mukherjee K, Majumder S, Mondal P K, and Deb B 2018 *J. Phys. B* **51** 015004
- [27] Wang J, Gacesa M and Cote R 2015 *Phys. Rev. Lett.* **114** 243003
- [28] Kumar T, Bhattacharjee A B and Manmohan 2011 *Int. J. Mod. Phys. B* **25** 1737
- [29] Hsueh C H, Tsai Y C, Wu K S, Chang M S and Wu W C 2013 *Phys. Rev. A* **88** 043646
- [30] Mauger S, Millen J and Jones M P A 2007 *J. Phys. B* **40** F319
- [31] Mcquillen P, Zhang X, Strickler T, Dunning F B and Killian T C 2013 *Phys. Rev. A* **87** 013407
- [32] Fields G, Zhang X, Dunning F B, Yoshida S and B 2018 *Phys. Rev. A* **97** 013429
- [33] Kartashov Y V, Malomed B A, Vysloukh V A and Torner L 2009 *Phys. Rev. A* **80** 053816
- [34] Cerda S C, Cavalcanti S B and Hickmann J M 1998 *Eur. Phys. J. D* **1** 313
- [35] Li H, Xu S L, Belić M R and Cheng J X 2018 *Phys. Rev. A* **98** 033827
- [36] Kartashov Y V, Malomed B A, Leticia T and Lluís T 2018 *Phys. Rev. A* **98** 013612
- [37] Murray C and Pohl T 2016 *Adv. At. Mol. Opt. Phys.* **65** 321
- [38] Kartashov Y V, Hang C, Huang G and Torner L 2016 *Optica* **3** 1048
- [39] Xu S L, Li H, Zhou Q, Zhou G P, Zhao D, Belić M R, He J R and Zhao Y 2020 *Opt. Express* **28** 16322
- [40] Novikova I, Phillips N B and Gorshkov A V 2008 *Phys. Rev. A* **78** 021802

Supplementary Material: Vector Spatiotemporal Solitons and Their Memory Features in Cold Rydberg Gases

Yuan Zhao (赵元)¹, Yun-Bin Lei (雷允彬)¹, Yu-Xi Xu (徐羽茜)², Si-Liu Xu (徐四六)^{1*}, Houria Triki³, Anjan Biswas^{4,5}, and Qin Zhou (周勤)^{6*}

¹School of Electronic and Information Engineering, Hubei University of Science and Technology, Xianning 437100, China

²School of International Education, Wuhan University of Technology, Wuhan, 430071, China

³Radiation Physics Laboratory, Department of Physics, Faculty of Sciences, Badji Mokhtar University, P. O. Box 12, 23000 Annaba, Algeria

⁴Department of Physics, Chemistry and Mathematics, Alabama A&M University, Normal, AL 35762-4900, USA

⁵Mathematical Modeling and Applied Computation (MMAC) Research Group, Department of Mathematics, King Abdulaziz University, Jeddah 21589, Saudi Arabia

⁶School of Mathematical and Physical Sciences, Wuhan Textile University, Wuhan, 430200, China

*Corresponding authors. Email: xusiliu1968@163.com(Siliu Xu) and qinzhou@whu.edu.cn (Qin Zhou)

Text A: Expansion equations of optical Bloch equation

The density equations ρ of the system is obtained by substituting the Hamiltonian to the optical Bloch equation $i\partial\rho/\partial t = -i[\hat{H}, \rho]/\hbar - \Gamma[\rho]$. For the 5×5 density matrix, we get the following expansion equations of optical Bloch equation.

$$i\left(\frac{\partial}{\partial t} + \Gamma_{21} + \Gamma_{31}\right)\rho_{11} - i(\Gamma_{12}\rho_{22} + \Gamma_{13}\rho_{33} + \Gamma_{14}\rho_{44}) - \Omega_p\rho_{41}^* + \Omega_p^*\rho_{41} = 0, \quad (\text{A1})$$

$$i\left(\frac{\partial}{\partial t} + \Gamma_{12}\right)\rho_{22} - i(\Gamma_{21}\rho_{11} + \Gamma_{24}\rho_{44}) - \Omega_s\rho_{42}^* + \Omega_s^*\rho_{42} = 0, \quad (\text{A2})$$

$$i\left(\frac{\partial}{\partial t} + \Gamma_{13}\right)\rho_{33} - i(\Gamma_{31}\rho_{11} + \Gamma_{34}\rho_{44}) - \Omega_c\rho_{43}^* + \Omega_c^*\rho_{43} = 0, \quad (\text{A3})$$

$$i\left(\frac{\partial}{\partial t} + \Gamma_{14} + \Gamma_{24} + \Gamma_{34}\right)\rho_{44} - i\Gamma_{45}\rho_{55} + \Omega_p\rho_{41}^* - \Omega_p^*\rho_{41} + \Omega_s\rho_{42}^* - \Omega_s^*\rho_{42} + \Omega_c\rho_{43}^* - \Omega_c^*\rho_{43} + \Omega_a\rho_{54}^* - \Omega_a^*\rho_{54} = 0, \quad (\text{A4})$$

$$i\left(\frac{\partial}{\partial t} + \Gamma_{45}\right)\rho_{55} - \Omega_a^*\rho_{54} + \Omega_a\rho_{45} = 0, \quad (\text{A5})$$

$$\left(i\frac{\partial}{\partial t} + d_{21}\right)\rho_{21} + \Omega_s^*\rho_{41} - \Omega_p\rho_{42}^* = 0, \quad (\text{A6})$$

$$\left(i\frac{\partial}{\partial t} + d_{31}\right)\rho_{31} + \Omega_c^*\rho_{41} - \Omega_p\rho_{43}^* = 0, \quad (\text{A7})$$

$$\left(i\frac{\partial}{\partial t} + d_{41}\right)\rho_{41} + \Omega_p(\rho_{11} - \rho_{44}) + \Omega_s\rho_{21} + \Omega_c\rho_{31} + \Omega_a^*\rho_{51} = 0, \quad (\text{A8})$$

$$\left(i\frac{\partial}{\partial t} + d_{51}\right)\rho_{51} + \Omega_a\rho_{41} - \Omega_p\rho_{54} - N_a \int d^3\mathbf{r}' V(\mathbf{r}' - \mathbf{r})\rho_{55,51}(\mathbf{r}', \mathbf{r}, t) = 0, \quad (\text{A9})$$

$$\left(i\frac{\partial}{\partial t} + d_{32}\right)\rho_{32} + \Omega_c^*\rho_{42} - \Omega_s\rho_{43}^* = 0, \quad (\text{A10})$$

$$\left(i\frac{\partial}{\partial t} + d_{42}\right)\rho_{42} + \Omega_s(\rho_{22} - \rho_{44}) + \Omega_p\rho_{21}^* + \Omega_c\rho_{32} + \Omega_a^*\rho_{52} = 0, \quad (\text{A11})$$

$$(i \frac{\partial}{\partial t} + d_{52})\rho_{52} + \Omega_a \rho_{42} - \Omega_s \rho_{54} - N_a \int d^3 \mathbf{r}' V(\mathbf{r}' - \mathbf{r}) \rho_{55,52}(\mathbf{r}', \mathbf{r}, t) = 0, \quad (\text{A12})$$

$$(i \frac{\partial}{\partial t} + d_{43})\rho_{43} + \Omega_c (\rho_{33} - \rho_{44}) + \Omega_s \rho_{32}^* + \Omega_p \rho_{31}^* + \Omega_a^* \rho_{53} = 0, \quad (\text{A13})$$

$$(i \frac{\partial}{\partial t} + d_{53})\rho_{53} + \Omega_a \rho_{43} - \Omega_c \rho_{54} - N_a \int d^3 \mathbf{r}' V(\mathbf{r}' - \mathbf{r}) \rho_{55,53}(\mathbf{r}', \mathbf{r}, t) = 0, \quad (\text{A14})$$

$$(i \frac{\partial}{\partial t} + d_{54})\rho_{54} + \Omega_a (\rho_{44} - \rho_{55}) - \Omega_p^* \rho_{51} - \Omega_s^* \rho_{52} - \Omega_c^* \rho_{53} - N_a \int d^3 \mathbf{r}' V(\mathbf{r}' - \mathbf{r}) \rho_{55,54}(\mathbf{r}', \mathbf{r}, t) = 0, \quad (\text{A15})$$

where $d_{jl} = \Delta_j - \Delta_l + i\gamma_{jl}$ ($i, j = 1, 2, 3, 4; i \neq j$), and $\gamma_{jl} = (\Gamma_j + \Gamma_l)/2 + \gamma_{ij}^{dep}$ with $\Gamma_l = \sum_{j < l} \Gamma_{jl}$.

Here Γ_{jl} denotes the spontaneous emission decay rate between states $|j\rangle$ and $|l\rangle$, and γ_{ij}^{dep} is the dephasing rate between the states $|j\rangle$ and $|l\rangle$.

Text B: Expansion equations of zeroth order density matrix elements and the first order solutions

(i) At the zeroth ($m = 0$) order, equations for $\rho_{32}^{(0)}, \rho_{42}^{(0)}, \rho_{43}^{(0)}, \rho_{52}^{(0)}, \rho_{53}^{(0)}$, and $\rho_{54}^{(0)}$ are given by

$$\begin{bmatrix} d_{32} & \Omega_c^* & 0 & 0 & 0 & 0 \\ \Omega_c & d_{42} & 0 & \Omega_a^* & 0 & 0 \\ 0 & 0 & d_{43} & 0 & \Omega_a^* & 0 \\ 0 & \Omega_a & 0 & d_{52} & 0 & 0 \\ 0 & 0 & \Omega_a & 0 & d_{53} & 0 \\ 0 & 0 & 0 & 0 & -\Omega_c^* & d_{54} \end{bmatrix} \begin{bmatrix} \rho_{32}^{(0)} \\ \rho_{42}^{(0)} \\ \rho_{43}^{(0)} \\ \rho_{52}^{(0)} \\ \rho_{53}^{(0)} \\ \rho_{54}^{(0)} \end{bmatrix} = \begin{bmatrix} 0 \\ 0 \\ \Omega_c (\rho_{44}^{(0)} - \rho_{33}^{(0)}) \\ 0 \\ 0 \\ -\Omega_a \rho_{44}^{(0)} \end{bmatrix}, \quad (\text{B1})$$

Equations for $\rho_{11}^{(0)}, \rho_{22}^{(0)}, \rho_{33}^{(0)}$, and $\rho_{44}^{(0)}$ read

$$\begin{bmatrix} -(\Gamma_{21} + \Gamma_{31}) & \Gamma_{12} & \Gamma_{13} & \Gamma_{14} \\ \Gamma_{21} & -\Gamma_{12} & 0 & \Gamma_{24} \\ \Gamma_{31} & 0 & -\Gamma_{13} & \Gamma_{34} \\ 1 & 1 & 1 & 1 \end{bmatrix} \begin{bmatrix} \rho_{11}^{(0)} \\ \rho_{22}^{(0)} \\ \rho_{33}^{(0)} \\ \rho_{44}^{(0)} \end{bmatrix} = \begin{bmatrix} 0 \\ 0 \\ i(\Omega_c \rho_{43}^{*(0)} - \Omega_c^* \rho_{43}^{(0)}) \\ 1 \end{bmatrix}, \quad (\text{B2})$$

And $\rho_{31}^{(0)} = \rho_{21}^{(0)} = \rho_{41}^{(0)} = \rho_{51}^{(0)} = 0, \rho_{32}^{(0)} = \rho_{42}^{(0)} = \rho_{52}^{(0)} = \rho_{55}^{(0)} = 0$.

(ii) At the first ($m = 1$) order, the solution for nonzero matrix elements reads

$$\rho_{31}^{(1)} = -\frac{\Omega_c^* (\omega + d_{21})(\omega + d_{31})(\rho_{11}^{(0)} - \rho_{44}^{(0)}) + |\Omega_c|^2 \rho_{43}^{*(0)}}{D_1} F_1 e^{i\theta_p} = a_{31}^{(1)} F_1 e^{i\theta_p} \quad (\text{B3})$$

$$\rho_{41}^{(1)} = \frac{(\omega + d_{21})(\omega + d_{31})(\rho_{11}^{(0)} - \rho_{44}^{(0)}) + \Omega_c \rho_{43}^{*(0)}}{D_1} F_1 e^{i\theta_p} = a_{41}^{(1)} F_1 e^{i\theta_p} \quad (\text{B4})$$

$$\rho_{51}^{(1)} = -\frac{\Omega_a (\omega + d_{21})(\omega + d_{31})(\rho_{11}^{(0)} - \rho_{44}^{(0)}) + \Omega_a \Omega_c \rho_{43}^{*(0)}}{D_1} F_1 e^{i\theta_p} = a_{51}^{(1)} F_1 e^{i\theta_p} \quad (\text{B5})$$

$$\rho_{32}^{(1)} = -\frac{\Omega_c^* (\omega + d_{32})(\omega + d_{52})(\rho_{22}^{(0)} - \rho_{44}^{(0)}) + (\omega + d_{32}) \Omega_a^* \Omega_c^* \rho_{54}^{(0)} + (\omega + d_{52}) |\Omega_c|^2 \rho_{43}^{*(0)}}{D_2} F_2 e^{i\theta_s} = a_{32}^{(1)} F_2 e^{i\theta_s} \quad (\text{B6})$$

$$\rho_{42}^{(1)} = \frac{(\omega + d_{32})(\omega + d_{52})(\rho_{22}^{(0)} - \rho_{44}^{(0)}) + (\omega + d_{32})\Omega_a^* \rho_{54}^{(0)} + (\omega + d_{52})\Omega_c \rho_{43}^{*(0)}}{D_2(\omega + d_{32})} F_2 e^{i\theta_s} = a_{42}^{(1)} F_2 e^{i\theta_s}, \quad (\text{B7})$$

$$\rho_{52}^{(1)} = -\frac{\Omega_a(\omega + d_{32})(\omega + d_{52})(\rho_{22}^{(0)} - \rho_{44}^{(0)}) + (\omega + d_{32})|\Omega_a|^2 \rho_{54}^{(0)} + (\omega + d_{52})\Omega_c \Omega_a \rho_{43}^{*(0)}}{D_2(\omega + d_{52})} F_2 e^{i\theta_s} = a_{52}^{(1)} F_2 e^{i\theta_s}, \quad (\text{B8})$$

with other $\rho_{jl}^{(1)} = 0$.

Text C: The second order solution

At the second order, the solution for nonzero matrix elements reads

$$\rho_{21}^{(2)} = \frac{1}{\omega + d_{21}} (\rho_{42}^{*(1)} F_1 e^{i\theta_p} - \rho_{41}^{(1)} F_2^* e^{-i\theta_s^*}), \quad (\text{C1})$$

$$\rho_{31}^{(2)} = \frac{-1}{\omega + d_{31}} (\Omega_c^* \rho_{41}^{(2)} + i a_{31}^{(1)}) \frac{\partial}{\partial t_1} F_1 e^{i\theta_p}, \quad (\text{C2})$$

$$\rho_{41}^{(2)} = \frac{i \left[(\omega + d_{31})(\omega + d_{51}) a_{41}^{(1)} + (\omega + d_{51}) \Omega_c a_{31}^{(1)} - (\omega + d_{31}) \Omega_a^* \rho_{51}^{(1)} \right]}{D_1} \frac{\partial}{\partial t_1} F_1 e^{i\theta_p}, \quad (\text{C3})$$

$$\rho_{51}^{(2)} = \frac{-1}{\omega + d_{31}} (\Omega_a a_{41}^{(2)} + i a_{51}^{(1)}) \frac{\partial}{\partial t_1} F_1 e^{i\theta_p}, \quad (\text{C4})$$

$$\rho_{32}^{(2)} = \frac{-1}{\omega + d_{32}} (\Omega_c^* \rho_{42}^{(2)} + i a_{32}^{(1)}) \frac{\partial}{\partial t_1} F_2 e^{i\theta_s}, \quad (\text{C5})$$

$$\rho_{42}^{(2)} = \frac{i \left[(\omega + d_{32})(\omega + d_{52}) a_{42}^{(1)} - (\omega + d_{52}) \Omega_c a_{32}^{(1)} - (\omega + d_{32}) \Omega_a^* \rho_{52}^{(1)} \right]}{D_2} \frac{\partial}{\partial t_1} F_2 e^{i\theta_s}, \quad (\text{C6})$$

$$\rho_{52}^{(2)} = \frac{-1}{\omega + d_{52}} (\Omega_a a_{42}^{(2)} + i a_{52}^{(1)}) \frac{\partial}{\partial t_1} F_2 e^{i\theta_s}, \quad (\text{C7})$$

$$\rho_{11}^{(2)} = a_{111}^{(2)} |F_1|^2 e^{(-2\bar{\alpha}_1 z_2)} + a_{112}^{(2)} |F_2|^2 e^{(-2\bar{\alpha}_2 z_2)}, \quad (\text{C8})$$

$$\rho_{22}^{(2)} = a_{221}^{(2)} |F_1|^2 e^{(-2\bar{\alpha}_1 z_2)} + a_{222}^{(2)} |F_2|^2 e^{(-2\bar{\alpha}_2 z_2)}, \quad (\text{C9})$$

$$\rho_{33}^{(2)} = a_{331}^{(2)} |F_1|^2 e^{(-2\bar{\alpha}_1 z_2)} + a_{332}^{(2)} |F_2|^2 e^{(-2\bar{\alpha}_2 z_2)}, \quad (\text{C10})$$

$$\rho_{44}^{(2)} = a_{441}^{(2)} |F_1|^2 e^{(-2\bar{\alpha}_1 z_2)} + a_{442}^{(2)} |F_2|^2 e^{(-2\bar{\alpha}_2 z_2)}, \quad (\text{C11})$$

$$\rho_{43}^{(2)} = a_{431}^{(2)} |F_1|^2 e^{(-2\bar{\alpha}_1 z_2)} + a_{432}^{(2)} |F_2|^2 e^{(-2\bar{\alpha}_2 z_2)}, \quad (\text{C12})$$

$$\rho_{53}^{(2)} = a_{531}^{(2)} |F_1|^2 e^{(-2\bar{\alpha}_1 z_2)} + a_{532}^{(2)} |F_2|^2 e^{(-2\bar{\alpha}_2 z_2)}, \quad (\text{C13})$$

$$\rho_{54}^{(2)} = a_{541}^{(2)} |F_1|^2 e^{(-2\bar{\alpha}_1 z_2)} + a_{542}^{(2)} |F_2|^2 e^{(-2\bar{\alpha}_2 z_2)}, \quad (\text{C14})$$

with

$$a_{111}^{(2)} = -\frac{(2A_1 + 2C_{11} + H_{11})X_1 - (A_1 + C_{11})\Gamma_{12}\Gamma_{13}\Gamma_{45} + C_{11}X_3 - A_1(\Gamma_{13}\Gamma_{24} + \Gamma_{12}\Gamma_{34})\Gamma_{45}}{X_2}$$

$$a_{112}^{(2)} = -\frac{(2B_1 + 2C_{12} + H_{12})X_1 - (B_1 + C_{12})\Gamma_{12}\Gamma_{13}\Gamma_{45} + C_{12}X_3 + B_1X_4}{X_2}$$

$$a_{221}^{(2)} = -\frac{(2A_1 + 2C_{11} + H_{11})Y_1 + A_1X_5 + C_{11}X_6}{X_2}$$

$$a_{222}^{(2)} = -\frac{(2B_1 + 2C_{12} + H_{12})Y_1 - B_1[Y_2 + (\Gamma_{21}\Gamma_{34} + \Gamma_{13}\Gamma_{21})\Gamma_{45}] + C_{12}X_6}{X_2}$$

$$a_{331}^{(2)} = -\frac{(2A_1 + 2C_{11} + H_{11})Z_1 - C_{11}[Z_2 + (\Gamma_{12} + \Gamma_{24})\Gamma_{31}\Gamma_{45}] + A_1X_7}{X_3}$$

$$a_{332}^{(2)} = -\frac{(2B_1 + 2C_{12} + H_{12})Z_1 - C_{12}[Z_2 + (\Gamma_{12} + \Gamma_{24})\Gamma_{31}\Gamma_{45}] + B_1(Z_3 - \Gamma_{12}\Gamma_{31}\Gamma_{45})}{X_3}$$

$$a_{431}^{(2)} = \frac{(\omega + d_{53}) \left[|\Omega_a|^2 \Omega_c (a_{111}^{(2)} - a_{221}^{(2)} - a_{331}^{(2)} - 2a_{441}^{(2)}) - D_4 \Omega_c (a_{331}^{(2)} - a_{441}^{(2)}) - \Omega_a \Omega_c^* a_{51}^{(1)} - D_4 a_{31}^{*(1)} \right]}{D_3 D_4 - |\Omega_a|^2 |\Omega_c|^2}$$

$$a_{432}^{(2)} = \frac{(\omega + d_{53}) \left[|\Omega_a|^2 \Omega_c (a_{112}^{(2)} - a_{222}^{(2)} - a_{332}^{(2)} - 2a_{442}^{(2)}) - D_4 \Omega_c (a_{332}^{(2)} - a_{442}^{(2)}) - \Omega_a \Omega_c^* a_{52}^{(1)} - D_4 a_{32}^{*(1)} \right]}{D_3 D_4 - |\Omega_a|^2 |\Omega_c|^2}$$

$$a_{531}^{(2)} = \frac{\Omega_a \left[|\Omega_a|^2 \Omega_c (a_{111}^{(2)} - a_{221}^{(2)} - a_{331}^{(2)} - 2a_{441}^{(2)}) - D_4 \Omega_c (a_{331}^{(2)} - a_{441}^{(2)}) - \Omega_a \Omega_c^* a_{51}^{(1)} - D_4 a_{31}^{*(1)} \right]}{D_3 D_4 - |\Omega_a|^2 |\Omega_c|^2}$$

$$-\frac{\left[\Omega_c a_{31}^{*(1)} - [\Omega_c]^2 (a_{331}^{(2)} - a_{441}^{(2)}) \right]}{\Omega_c \Omega_a^*} - \frac{D_4 a_{431}^{(2)}}{\Omega_a^* (\omega + d_{53})}$$

$$a_{532}^{(2)} = \frac{\Omega_a \left[|\Omega_a|^2 \Omega_c (a_{112}^{(2)} - a_{222}^{(2)} - a_{332}^{(2)} - 2a_{442}^{(2)}) - D_4 \Omega_c (a_{332}^{(2)} - a_{442}^{(2)}) - \Omega_a \Omega_c^* a_{52}^{(1)} - D_4 a_{32}^{*(1)} \right]}{D_3 D_4 - |\Omega_a|^2 |\Omega_c|^2}$$

$$+\frac{\left[\Omega_c a_{32}^{*(1)} - [\Omega_c]^2 (a_{332}^{(2)} - a_{442}^{(2)}) \right]}{\Omega_c \Omega_a^*} - \frac{D_4 a_{432}^{(2)}}{\Omega_a^* (\omega + d_{53})}$$

$$a_{541}^{(2)} = -\frac{(\omega + d_{53}) \left[\Omega_c (a_{331}^{(2)} - a_{441}^{(2)}) + a_{31}^{*(1)} \right] + D_4 a_{431}^{(2)}}{\Omega_c \Omega_a^*}$$

$$a_{542}^{(2)} = \frac{(\omega + d_{53}) \left[a_{32}^{*(1)} - \Omega_c (a_{332}^{(2)} - a_{442}^{(2)}) \right] - D_4 a_{432}^{(2)}}{\Omega_c \Omega_a^*}$$

where

$$A_1 = \frac{\Omega_c \rho_{43}^{*(0)} - \Omega_c^* \rho_{43}^{(0)}}{D_1}$$

$$B_1 = \frac{(\omega + d_{32}) (\Omega_a^* \rho_{54}^{(0)} - \Omega_a \rho_{54}^{*(0)}) + (\omega + d_{52}) (\Omega_c \rho_{43}^{*(0)} - \Omega_c^* \rho_{43}^{(0)})}{D_2}$$

$$C_{11} = \frac{(\omega + d_{53}) \left[[\Omega_c]^2 \Omega_a^* a_{51}^{*(1)} - \Omega_a [\Omega_c^*]^2 a_{51}^{(1)} + \Omega_c D_4 a_{31}^{(1)} - \Omega_c^* D_4 a_{31}^{*(1)} \right]}{D_3 D_4 - |\Omega_a|^2 |\Omega_c|^2}$$

$$C_{12} = \frac{(\omega + d_{53}) \left[|\Omega_c|^2 \Omega_a^* a_{52}^{*(1)} - \Omega_a \left[\Omega_c^* \right]^2 a_{52}^{(1)} + \Omega_c D_4 a_{32}^{(1)} - \Omega_c^* D_4 a_{32}^{*(1)} \right]}{D_3 D_4 - |\Omega_a|^2 |\Omega_c|^2}$$

$$D_3 = (\omega + d_{53})(\omega + d_{43}) - |\Omega_a|^2$$

$$D_4 = (\omega + d_{53})(\omega + d_{54}) - |\Omega_c|^2$$

$$H_{11} = \frac{D_4(\omega + d_{54})}{D_3 D_4 - |\Omega_a|^2 |\Omega_c|^2} \left[\frac{\Omega_c^* \Omega_a a_{51}^{(1)} + D_4 a_{31}^{*(1)}}{\Omega_c} - \frac{\Omega_a^* \Omega_c a_{51}^{*(1)} + D_4 a_{31}^{(1)}}{\Omega_c^*} \right] + (\omega + d_{53}) \left(\frac{a_{31}^{(1)}}{\Omega_c^*} - \frac{a_{31}^{*(1)}}{\Omega_c} \right)$$

$$H_{12} = \frac{D_4(\omega + d_{54})}{D_3 D_4 - |\Omega_a|^2 |\Omega_c|^2} \left[\frac{\Omega_c^* \Omega_a a_{52}^{(1)} + D_4 a_{32}^{*(1)}}{\Omega_c} - \frac{\Omega_a^* \Omega_c a_{52}^{*(1)} + D_4 a_{32}^{(1)}}{\Omega_c^*} \right] + (\omega + d_{53}) \left(\frac{a_{32}^{(1)}}{\Omega_c} - \frac{a_{32}^{*(1)}}{\Omega_c^*} \right)$$

$$X_1 = \Gamma_{12} \Gamma_{13} (\Gamma_{14} + \Gamma_{24} + \Gamma_{34})$$

$$X_2 = (\Gamma_{12} \Gamma_{13} + \Gamma_{21} \Gamma_{13} + \Gamma_{12} \Gamma_{31}) (\Gamma_{14} + \Gamma_{24} + \Gamma_{34}) \Gamma_{45}$$

$$X_3 = (\Gamma_{12} \Gamma_{14} + \Gamma_{12} \Gamma_{24} - \Gamma_{13} \Gamma_{24}) \Gamma_{45}$$

$$X_4 = (\Gamma_{13} \Gamma_{14} + \Gamma_{13} \Gamma_{34} - \Gamma_{12} \Gamma_{34}) \Gamma_{45}$$

$$X_5 = (\Gamma_{13} \Gamma_{24} + \Gamma_{24} \Gamma_{31} - \Gamma_{13} \Gamma_{21} - \Gamma_{34} \Gamma_{21}) \Gamma_{45}$$

$$X_6 = (\Gamma_{13} \Gamma_{24} + \Gamma_{24} \Gamma_{31} + \Gamma_{21} \Gamma_{24} - \Gamma_{13} \Gamma_{21} - \Gamma_{14} \Gamma_{21}) \Gamma_{45}$$

$$X_7 = (\Gamma_{12} \Gamma_{34} + \Gamma_{21} \Gamma_{34} - \Gamma_{24} \Gamma_{31} - \Gamma_{12} \Gamma_{31}) \Gamma_{45}$$

$$Y_1 = (\Gamma_{14} \Gamma_{21} + \Gamma_{24} \Gamma_{21} + \Gamma_{34} \Gamma_{21}) \Gamma_{13}$$

$$Y_2 = (\Gamma_{13} \Gamma_{14} + \Gamma_{14} \Gamma_{31} + \Gamma_{34} \Gamma_{13} + \Gamma_{34} \Gamma_{31}) \Gamma_{45}$$

$$Z_1 = (\Gamma_{14} + \Gamma_{24} + \Gamma_{34}) \Gamma_{12} \Gamma_{31}$$

$$Z_2 = (\Gamma_{14} \Gamma_{12} + \Gamma_{21} \Gamma_{14} + \Gamma_{12} \Gamma_{24} + \Gamma_{21} \Gamma_{24}) \Gamma_{45}$$

$$Z_3 = (\Gamma_{34} \Gamma_{12} + \Gamma_{21} \Gamma_{34} + \Gamma_{31} \Gamma_{14} + \Gamma_{31} \Gamma_{34}) \Gamma_{45}$$

Text D: Explicit expressions of W_{jl}

$$W_{11} = -\kappa_{14} \frac{\Omega_c (\omega + d_{51}) a_{431}^{*(2)} + \Omega_a^* (\omega + d_{31}) \rho_{541}^{(2)} + (\omega + d_{31})(\omega + d_{51})(a_{111}^{(2)} - a_{441}^{(2)})}{D_1}, \quad (D1)$$

$$W_{12} = -\kappa_{14} \frac{\Omega_c (\omega + d_{51}) a_{432}^{*(2)} + \Omega_a^* (\omega + d_{31}) \rho_{542}^{(2)} + (\omega + d_{31})(\omega + d_{51})(a_{112}^{(2)} - a_{442}^{(2)} + a_{21}^{(2)})}{D_1}, \quad (D2)$$

$$W_{21} = -\kappa_{24} \frac{\Omega_c (\omega + d_{52}) a_{431}^{*(2)} + \Omega_a^* (\omega + d_{32}) \rho_{541}^{(2)} + (\omega + d_{32})(\omega + d_{52})(a_{221}^{(2)} - a_{441}^{(2)} + a_{21}^{*(2)})}{D_2}, \quad (D3)$$

$$W_{22} = -\kappa_{24} \frac{\Omega_c (\omega + d_{52}) a_{432}^{*(2)} + \Omega_a^* (\omega + d_{32}) \rho_{542}^{(2)} + (\omega + d_{32})(\omega + d_{52})(a_{222}^{(2)} - a_{442}^{(2)})}{D_2}, \quad (D4)$$

where $a_{21}^{(2)} = (a_{42}^{*(1)} - a_{41}^{(1)}) / (\omega + d_{21})$.